

Portable Heating and Temperature-Monitoring System with a Textile Heater Embroidered on the Facemask

Mitar Simić,* Adrian K. Stavrakis, and Goran M. Stojanović

Cite This: *ACS Omega* 2022, 7, 47214–47224

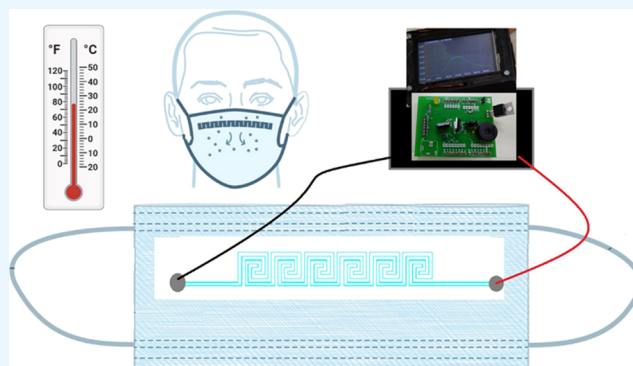
Read Online

ACCESS |

Metrics & More

Article Recommendations

ABSTRACT: Personal heating systems are getting increasing interest because of the need to reduce the negative impact of cold weather on the health of people and animals. Heating the air before inhalation is of great importance as it can reduce the probability of various diseases. In this paper, we present a textile-based heater composed of commercial conductive threads, embroidered on an ordinary protective facemask. We also present the design and implementation details of the temperature monitoring and controlling circuit. Air temperature inside the facemask was monitored by a thermocouple placed in close proximity to the nose (nostrils). Preliminary testing revealed that the difference among temperatures in repeated heating cycles is in the range of ± 1.5 °C. The response time for temperature increase from 29.9 to 40.5 °C was about 4 min, while the recovery time from 40.5 to 31.3 °C was about 4.3 min. Safety for human use and wireless data transmission to an application installed on a mobile phone are also demonstrated.



1. INTRODUCTION

Cold weather conditions are very harmful to people and animals, causing 240 hospital admissions and 15 deaths (1.8 per million) in New York, the largest city in the United States, from 2005 to 2014.¹ Diurnal temperature was identified as one of the serious contributing factors when it comes to stroke mortality in China² and Canada.³ A recent study has shown that the number of deaths caused by cold weather is significantly higher in the case of repetitive extreme cold weather events.⁴ A key takeout is that the majority of deaths and illnesses mostly occurs because of staying outside during the period of cold weather.¹ Therefore, there is an increasing demand for providing wearable and portable heating elements that will help people who stay outdoors overcome issues related to cold weather. If cold air is inhaled and it reaches the lungs, the human body responds by releasing histamine or other inflammatory mediators. In addition to that, the body also works to heat the inhaled air to 36–37 °C, which requires significant efforts and energy.⁵ Studies also show that human exposure to cold air without gradual adaptation can lead to a high risk of exacerbation of respiratory symptoms within a few hours or days.⁶

The realization of textile-based heating elements can offer a lot of advantages such as flexibility, compatibility with the body shape, and elimination of the need for carrying bulky elements as all parts can be integrated into the clothes and even decorated.^{7,8} For example, a thermal glove is an example of soft

and lightweight realization of the personal thermal management system.⁹ Moreover, textile-based coils enable wireless energy transfer which improves convenience for users.¹⁰ An example of a wearable textile heater is a belt with a heating element made from conductive ink presented in the study by Shahariar et al.¹¹ Another example of a wearable stretchable heater based on a silver nanowire composite is presented in the study by Wu et al.¹² The first realizations of a wearable stretchable heater based on silver nanowire composites are presented in the study by Hong et al.¹³ The presented solution is also transparent, which increases the user comfort. A MXene-based heater on a fiber substrate is shown in the study by Liu et al.,¹⁴ where the authors proposed the use of dip coating as the deposition technique, enabling flexibility and light-weight characteristics.¹⁴ Moreover, the MXene-based polyester textile heaters were also found to be water-resistant with additional features such as electromagnetic interference shielding.^{15,16} Particle-free silver inks are also an appropriate solution for the realization of heaters on textile substrates,

Received: October 5, 2022

Accepted: November 10, 2022

Published: December 7, 2022



exhibiting good thermal stability.¹⁷ Poly(vinyl alcohol) nanocomposite fibers also showed high thermal stability in integration with textiles for realizations of heating elements.¹⁸ Graphene-based thermal elements are highly conductive and flexible, making them a very promising element for personalized electronic healthcare systems.¹⁹ A wearable textile-based conductive strip, based on the polymer composites, is also a very interesting heating element with excellent one-dimensional stretchability and hydrophobic properties.²⁰ In addition to the silver conductive inks, MXene, graphene, and conductive polymers, recent studies have shown excellent heating properties of carbon fabric^{21,22} and carbon-based conductive inks for low voltage heaters.²³ A carbon-based flexible printed wearable heater is also represented in the study by Salam et al.²⁴

Even though the abovementioned realizations of textile-based heaters showed promising features for the future of the electronic textile (e-textile) structures, their main disadvantage is the complexity of the fabrication process, as they require bulky and costly equipment for the deposition of conductive inks. In this paper, we present the methodology of the textile heaters based on commercial conductive (silver-plated) threads that are embroidered onto an ordinary facemask. All components of the system are commercially available, which eliminates the need for a complex and expensive production process, reducing the cost and enabling wide use. To the best of our knowledge, this is the first such realization ever reported. Because of the spread of the COVID-19 pandemic in 2020, wide use of protective facemasks was started worldwide, and people got used to them over time. Facemasks were also found to be an appropriate medium for the deployment of air filters for thermal sterilization against *E. coli* and *G. anodireducens*,²⁵ as well as dynamic pore modulation of stretchable air filters for machine-learned adaptive face masks.²⁶ Moreover, a recent study showed that viral inactivation by heating at 90 °C can limit transmission to a 3-log reduction level.²⁷ In addition to their health-protective purpose, facemasks also have an important role in cold weather areas where athletes can use them during outdoor activities, as well as workers in cold storages, and so forth. Textile heaters based on the silver threads embroidered on the facemask offer advantages in terms of the very simple fabrication process, low cost, easy fitting to a stable position that does not change during motion, and antibacterial properties of silver that make safe the contact with the human skin.²⁸ Moreover, additional sensing opportunities are possible with sensor integration to the facemask, such as capacitive respiration monitoring sensors embroidered to an ordinary facemask.²⁹

This paper is organized as follows: the overall system architecture description is decomposed to its main elements and described in Section 2, with provided details about the textile heater, temperature monitoring and controlling circuit, as well as data acquisition system. The main experimental results are provided in Section 3. The complete heating system was initially tested with the facemask mounted on the adult mannequin (mannequin model), which was followed by tests with a human volunteer. The conclusion and discussion about the future works are given in Section 4.

2. METHODS AND MATERIALS

2.1. System Architecture. The overall system architecture is shown in Figure 1. The core of the electronics part is a microcontroller board that provides commands to the

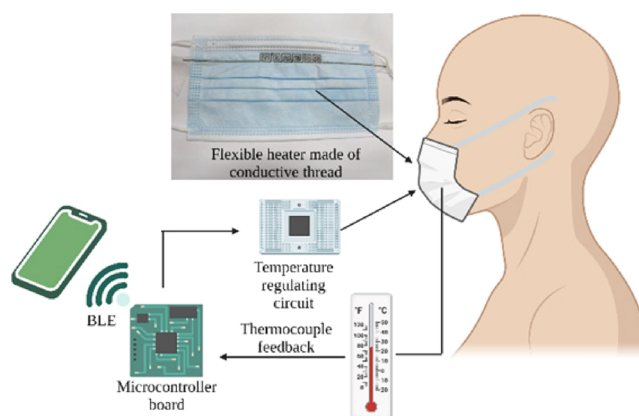


Figure 1. Overall system architecture.

temperature regulating circuit as well as performs the readout of the temperature of the air between the nose and facemask. It is also responsible for wireless data transmission over a Bluetooth Low Energy (BLE) link to the mobile phone. With a dedicated application, it is possible to get information about the actual temperature of the air inside the facemask with the embroidered textile heating element.

2.2. Textile Heater Embroidered to the Facemask. A textile-based heater was embroidered onto the inner side of a protective facemask. The basic heater topology was designed in AutoCAD2021, with main dimensions in mm shown in Figure 2. The conductive thread applied was the Silver-Tech+100

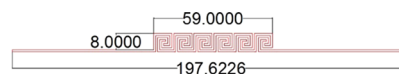


Figure 2. Design specifications and dimensions in millimeters of the embroidered textile heater.

silver-coated polyamide conductive thread produced by the AMANN Group (Bönningheim, Germany), with a nominal resistance of less than 200 Ω/m. The actual resistance of the thread is not provided by the manufacturer, as the fabrication procedure results in threads, the resistance of which varies within some range.²⁸ Tex size of the Silver-Tech+100 silver-coated polyamide conductive thread is 33, while the appropriate needle size is 75–90 number metric (Nm). Therefore, the thread diameter is expected to be smaller than 0.75–0.9 mm. The total length of the conductive thread needed to embroider the design from Figure 2 is about 11 m. With the price from the local distributor³⁰ of 45 EUR/km, the total price of the consumables for heater realization is less than 0.5 EUR. The total weight of the heater structure is less than 3 g. Embroidering of the heater was performed using the JCZA 0109 (ZSK, Germany) technical embroidery machine. The digital vector file from the design software was converted into a machine stitch file using the proprietary software of the embroidery machine. As an underside (bobbin), a typical polyester white thread with weight 150 was used, supplied by Madeira, U.K.

The heater design (Figure 2) occupies an area of 1817.9 mm², while the proposed embroidery form makes in total 2729 stitches, with distances from 0.4 to 4.4 mm. Such an approach results in a very robust structure that is not expected to have broken parts of the conductive threads during the normal use. Our experimental work confirmed that, as during the use in

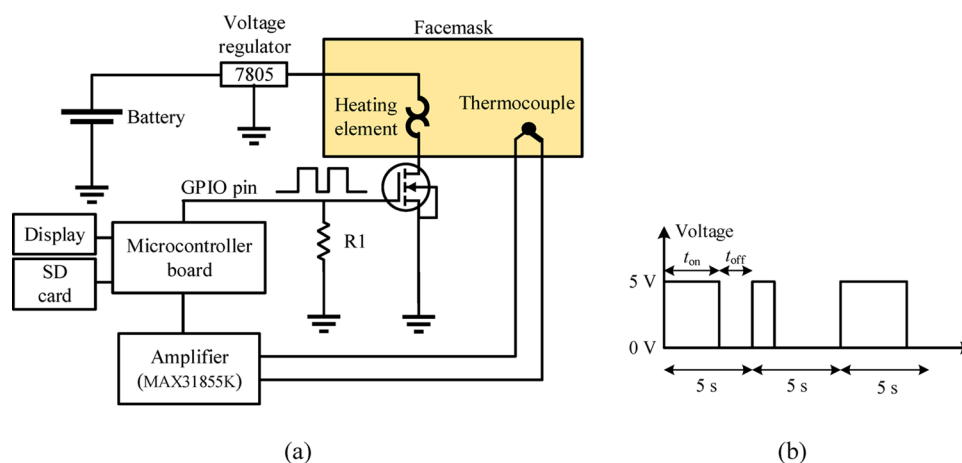


Figure 3. (a) Temperature regulating circuit and (b) temperature regulating diagram.

tests described in this paper, no changes in heater structures and performances were noticed.

When used as heaters embroidered to the facemask, the conductive threads are exposed to moisture and temperature changes. However, our recent study showed the suitability of conductive threads to be used as moisture sensors, with stable characteristics with moisture levels up to 50 μL of water, as well as artificial sweet and blood serum.³¹

Because of the fact that embroidery strikes a delicate balance between the top and bottom thread tensions, the conditions and appropriateness of the needle, the tension of the backing fabric on the embroidery field, and the overall fabric stability, an allowable tolerance of approximately ± 0.2 mm was applied to all dimensions, as shown in Figure 2.

2.3. Temperature Regulation Circuit. The temperature-regulating circuit is shown in Figure 3a. A battery is connected to the input of a voltage regulator IC7805, and stable 5 V output is provided to one end of the textile heater. Voltage regulation of the IC7805 is typically in the range of 5–50 mV. The use of a battery was proposed to ensure portable operation. The 5 V output level was chosen as it is recently considered as the gold standard for many mobile applications and because it easily can be obtained using the USB protocol or devices such as power banks, for example. The voltage regulator IC7805 also has bypass capacitors of 10 μF and 100 nF connected to its input and output pins, respectively. The other end of the heater is connected to the drain of a metal-oxide silicon field effect transistor (MOSFET) (IRLZ44Z), the gate of which is switched on/off by the microcontroller through a general-purpose input–output (GPIO) pin defined as the digital output. A gate threshold voltage of IRLZ44Z is in the range from 1 to 3 V. The air temperature inside the facemask is obtained by a K-type thermocouple. Amplification and cold-compensation reference for the thermocouple is provided using a separate circuit based on the integrated circuit MAX31855K. A real-time graph of the measured temperature values is presented locally on a thin-film-transistor liquid-crystal display. For demonstration purposes, the air temperature (set value) inside the facemask was selected to be regulated in the range 40–44 $^{\circ}\text{C}$. This range was selected based on the estimation about providing pleasant conditions during cold weather, but it can be changed according to user preferences. Moreover, experiments presented in the study by Payne-James et al.³² revealed that skin burns and tissue injuries will not occur at temperatures below 44 $^{\circ}\text{C}$. At 44 $^{\circ}\text{C}$ or

slightly above, injuries will occur after several hours, as summarized in Table 1.³²

Table 1. Contact Time with Temperatures That Cause Partial-Thickness Burns³²

temperature ($^{\circ}\text{C}$)	required contact time
45 $^{\circ}\text{C}$	3 h
50 $^{\circ}\text{C}$	4 min
55 $^{\circ}\text{C}$	30 s
60 $^{\circ}\text{C}$	5 s
65 $^{\circ}\text{C}$	1 s

In Section 3, we showed that range of temperatures 40–44 $^{\circ}\text{C}$ can be achieved with an appropriate selection of voltage applied on the heater. For example, a recent study showed that wearing a facemask with a heated barrier with temperature above 40 $^{\circ}\text{C}$ can help in killing viruses.³³ Our current realization allows us to define the temperature set value only during microcontroller programming, but we will include a manual update and configuration of the set value in future work.

The heating process starts with setting the GPIO pin to High (logical 1). After that, the air temperature inside the mask is measured using the thermocouple, and based on that value, the microcontroller decides for how long the MOSFET will be switched on or off, by controlling the ratio of the $t_{\text{on}}/t_{\text{off}}$ phases during a 5 s interval, as shown in Figure 3b. The time interval of 5 s was defined with the goal to provide a fast response but also good temperature control with a small overshoot, and it is validated by experimental testing. However, the length of the time interval can be changed if in later testing we find a more optimal value.

The timing of the circuit control is summarized in Table 2. If the air temperature measured by the thermocouple is lower than 46 $^{\circ}\text{C}$, the heater is turned on as it is required to provide additional heat to increase air temperature. If it is higher than the given threshold (46 $^{\circ}\text{C}$), based on the fact that higher temperatures can cause discomfort and lead to burns, the heater is switched off. The ratio of $t_{\text{on}}/t_{\text{off}}$ phases is defined with an aim to provide temperature regulation. For example, if the actual air temperature is lower than 25 $^{\circ}\text{C}$, then the heater is turned on for the complete duration of the 5 s cycle. It is important to notice that the given temperature T in Table 2 is not a set value (wanted temperature) or the heater

Table 2. Timing of the On/Off Phases Based on the Actual Temperature inside the Facemask

measured air temperature T	t_{on} (s)	t_{off} (s)	heater status
$<25\text{ }^{\circ}\text{C}$	5.0	0.0	on
$25\text{ }^{\circ}\text{C} < T < 30\text{ }^{\circ}\text{C}$	4.5	0.5	on
$30\text{ }^{\circ}\text{C} < T < 35\text{ }^{\circ}\text{C}$	3.5	1.5	on
$35\text{ }^{\circ}\text{C} < T < 44\text{ }^{\circ}\text{C}$	2.0	3.0	on
$44\text{ }^{\circ}\text{C} < T < 46\text{ }^{\circ}\text{C}$	0.5	4.5	on
$>46\text{ }^{\circ}\text{C}$	0.0	5.0	off

temperature, but it is air temperature measured by the thermocouple.

2.4. Data Acquisition. The data acquisition process can be performed in three ways. First, information about the measured temperature and the t_{on} value is saved in the form of a text file on the SD card, connected to the microcontroller

through the Serial Peripheral Interface (SPI). The second option is to use the universal serial bus (USB) to transfer data to the PC. Additionally, wireless data transmission to a mobile phone can be performed using the BLE link. The used BLE module is nRF24L01 from Nordic Semiconductors configured to work in broadcast mode, which means that is only required to have a mobile phone with the installed Android application to get the actual air temperature inside the mask.

3. EXPERIMENTAL RESULTS AND DISCUSSION

3.1. Hardware Realization of the System. The same heater topology was embroidered on 10 facemasks that were used for testing. Both the inner and outer facemask sides with the embroidered heating element are shown in Figure 4a. Embroidered heaters were first analyzed under a microscope with an aim to verify the shape and structure of the conductive patterns (inset of Figure 4a) in order to avoid any defects such

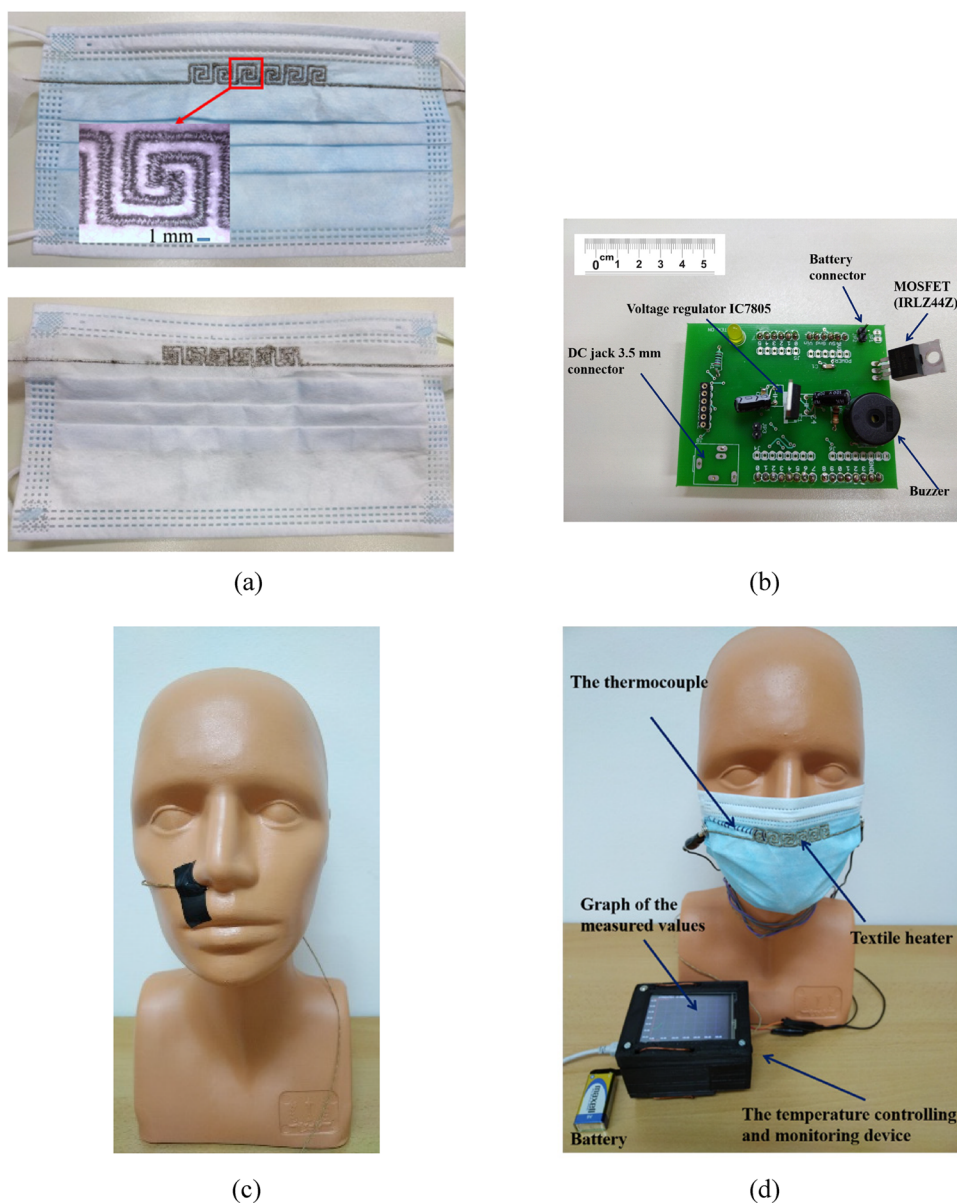


Figure 4. (a) Hardware realization of the textile heater embroidered to the facemask: external (top part) and internal sides (bottom part), (b) hardware realization of the temperature-regulating and -monitoring circuit, (c) thermocouple position, and (d) hardware realization of the temperature-controlling and -monitoring device and connection with the thermocouple.

as attachment of two neighboring segments or partial contact of rogue thread trimmings which can cause an uneven resistance profile of the heater element.

Hardware realization of the temperature-controlling and -monitoring circuit is shown in Figure 4b. As it can be seen from Figure 4b, it was designed in such a form factor to allow easy integration with Arduino boards. For example, in this study, we used Arduino Uno Board which is based on the ATmega328P microcontroller.

The thermocouple was positioned very close to the nose, as shown in Figure 4c. The textile heater was connected via crocodile clips to the temperature-controlling and -monitoring device (Figure 4d).

3.2. Electrical Impedance Spectroscopy Analysis. The mean and standard deviation of DC resistance R_{DC} (measured with Sanwa CD770 multimeter) of all 10 facemasks were first obtained as $27.2 \Omega \pm 1.3 \Omega$, with minimum and maximum values equal to 25.3 and 29.3 Ω , respectively. The actual values of resistance for each facemask are given in Table 3.

Table 3. Resistances R_{DC} and Average Values \pm Standard Deviations of Impedance Z in the Frequency Range from 1 Hz to 200 kHz for Each Facemask

no.	R_{DC} (Ω)	Z (Ω)
1	27.1	26.06 ± 0.02
2	26.5	27.28 ± 0.01
3	27.8	28.75 ± 0.01
4	25.9	25.39 ± 0.01
5	25.3	26.53 ± 0.01
6	29.3	29.31 ± 0.01
7	26.8	25.22 ± 0.01
8	26.3	25.74 ± 0.01
9	29.2	27.69 ± 0.01
10	28.1	26.39 ± 0.01

The heater structure was then characterized by using electrical impedance spectroscopy (EIS). The commercial impedance analyzer (HIOKI IM5982, Japan) was used to measure impedance in the frequency range from 1 Hz to 200 kHz (at 11 logarithmically spaced points). The average values and standard deviations of the impedance modulus (Z) of each facemask in the analyzed frequency range are also summarized in Table 3.

The importance of EIS in the case of the heaters is to provide information about the impedance stability of the conductive thread-based heater as well as the power factor ($\cos\phi$) calculation. As conductive materials have some parasitic inductance and capacitance, they will also have some conversion losses because of the reactive power (primarily in the form of lost on the transmission path). This intrinsic property of the embroidered heaters is not very significant in the case of DC-powered heaters. We included EIS analysis for a more comprehensive characterization and to aid our future plans for the developments of this study. The average values of the calculated power factor values are shown in Figure 5a, and they are indicating values very close to the ideal value of 1.0 for frequencies up to 100 kHz, promising a significant potential for AC-based heaters as well. Moreover, $\cos\phi$ values very close to 1.0 confirmed that the measured impedance is very close to the electrical resistance of the heaters, as shown in Table 3.

3.3. Testing and Monitoring of the Heating Process with the Mannequin Model. Initially, the heating structure was characterized with a constant heater voltage over a set period of time. The embroidered heater on the facemask was directly connected to the DC power supply (Siglent SPD3303C). The heater voltage was initially set to 1 V, and it was kept constant for 5 min, while the temperature inside the mask was monitored by the thermocouple. The DC power supply was then disconnected for 5 min, giving time for the

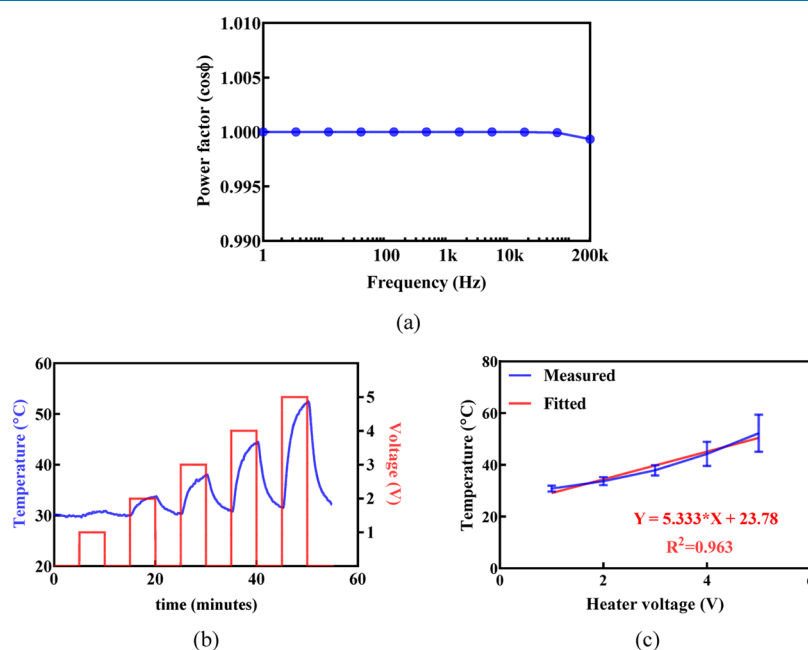


Figure 5. (a) Average values of the calculated power factor values for the 10 embroidered heaters in the frequency range from 1 Hz to 200 kHz. (b) Average values of the air temperature inside the facemasks for different values of the constant heater voltages over 5 min time period for all 10 heaters. (c) Calibration curve for the relationship between the air temperature inside the facemask and heater voltage levels at the end of the 5 min time period.

heater to cool down, and to reach the initial ambient temperature again. Voltage was then increased to 2 V, and the procedure was repeated, followed by the procedure with voltage values of 3, 4, and 5 V. The room temperature was regulated at (29 ± 2) °C with a commercial air conditioner. We did not choose to test our heaters in a thermal chamber as the developed system is intended to be used in an ambient environment, with expected fluctuations in the surrounding air temperature. Therefore, the performed characterization provides better performance evaluation in conditions that are expected to be present during the application. The average values of air temperature for all 10 facemasks are given in Figure 5b. The normalized standard deviation (standard deviation divided by the average value) was lower than 15%. As it can be seen from Figure 5b, there is no need for voltage increase over 5 V as air temperature higher than 40 °C can be obtained with 5 V in less than 2 min.

There is a gradual increase in air temperature with increased applied voltage on the heater. However, there are some differences between measured air temperature for different masks, up to 15%. The primary reason for this can be attributed to the lack of a standard or unique way of placing the mask on the mannequin model, which may impact the distance between the heater and thermocouple. When the thermocouple is placed closer to the conductive thread, it will register a higher temperature because the air temperature decreases by increasing the distance from the heater. However, by measuring the intensity of the electrical current flowing through the heater during the experiments, we determined the average current consumption for all 10 heaters (Table 3). We compared these values with the calculated values (using the value of the applied voltage on the heater and DC resistance of the heater) shown in Table 4 as well. It is important to notice

Table 4. Summary of Electrical Performance

heater voltage (V)	1	2	3	4	5
measured current (A)	0.04	0.07	0.11	0.15	0.19
nominal current (A)	0.04	0.07	0.11	0.15	0.18
power (W)	0.04	0.14	0.33	0.6	0.95

that all 10 heaters had a very stable operation in terms of electrical performance, which means that dissipated heat energy from the heaters is repeatable among different facemasks.

With average values of temperature at the end of the time interval of 5 min for 10 facemasks (Figure 5b), we were able to infer a calibration curve that links the heater voltage and the air

temperature inside the facemasks. The obtained plots are given in Figure 5c. As it can be seen, R^2 is 0.963.

The second important characterization is related to the time–temperature relationship for the constant heater voltage. As it was expected, the highest value of the heater voltage (5 V) generated the fastest response and the highest temperature, which was the reason why we choose 5 V for the heater implementation circuit. Moreover, it is important to notice that air temperature can be increased much more than that needed for the given application ($40 \div 44$ °C) even with 5 V, which opens new avenues for future work and new applications of the proposed textile heating element.

The device was then tested in terms of air temperature regulation. It was turned on and the temperature was monitored until it was regulated to a stable value threshold ($40 \div 42$ °C). That state was maintained for approximately 10 min. Then, the battery was disconnected, but the temperature was monitored until it dropped to a value very close to the initial ambient temperature. The described procedure was repeated for a total of three cycles. The obtained values are labeled as Cycle #1, Cycle #2, and Cycle #3, as shown in Figure 6a. As it can be seen, there were very small variations between measured values in these three cycles (1.5 °C), indicating the repeatability of the delivered service with the proposed design. As it can be seen from Figure 6a, the initial temperature at the beginning of the different cycles can be slightly different, owing to ambient temperature changes. That is the reason why we performed the next test to verify that there is no impact of the initial temperature on the final value of the temperature.

The device was initially turned on until it reached a stable temperature ($T \approx 40$ °C). It was then switched off, and it was turned on when the temperature dropped below 37 °C. It was again switched off when it reached a stable temperature. The device was then switched off, and it was turned on when the temperature dropped below 34 °C. It was again switched off when it reached a stable temperature, and the temperature was monitored until it fell to the initial temperature. The temperature log, shown in Figure 6b, clearly indicates that the initial temperature does not have an impact on achieving the preset threshold, eliminating the influence of the environmental temperature as well.

The measured values from Cycle #2 were arbitrarily used to determine the response and recovery time of the embroidered heater with the implemented temperature regulation circuit. The obtained values for these are expected to be longer than the case of characterization without temperature regulation,

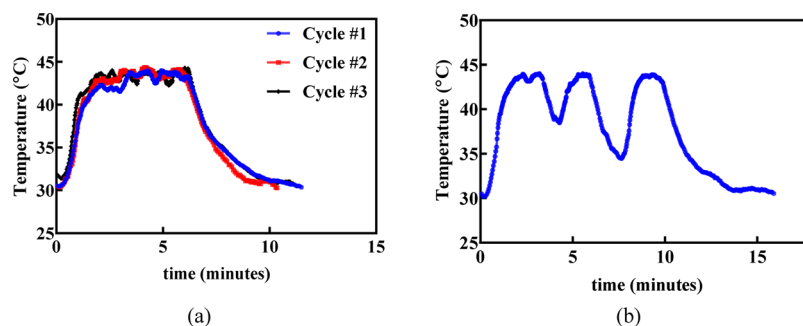


Figure 6. (a) Temperature values of the air inside the facemasks during three repeated cycles and (b) temperature values of the air inside the facemask for different initial temperatures.

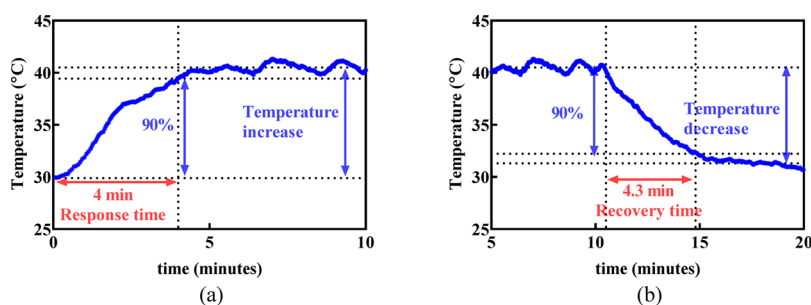


Figure 7. (a) Response time of the proposed heater and (b) recovery time of the fabricated heater.

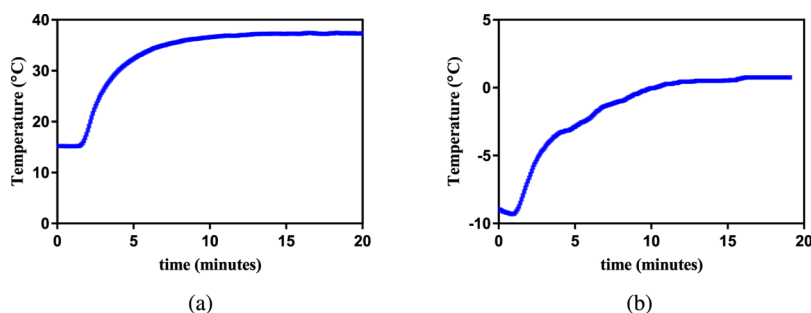


Figure 8. Temperature values of the air inside the facemask for different ambient temperatures: (a) 4–6 °C and (b) –18 °C.

but our goal was to characterize the system in a configuration as close as possible to its intended future use.

The response time was determined as the time interval required for the air temperature to reach 90% of the set threshold temperature (40.50 °C). The initial air temperature was 29.9 °C, and the response time was determined as 4 min, as shown in Figure 7a.

The recovery time was determined as the time interval required so that air temperature drops by 90% of the threshold temperature (to 31.3 °C) toward ambient temperature. The response time was determined as 4.3 min, as shown in Figure 7b.

It should be noticed that the temperature rise and fall time will be dependent on the mask type. In this work, we used a surgical single-use facemask which has great breathability, but as they are not in full contact with the human face, there are some considerable heat losses. Higher efficiency masks can be realized if there is a greater area that is in contact with skin, which will reduce heat loss in cold environments. However, this type of masks can be challenging to wear and can hinder the ability of normal speaking, and they will have contact with lips.

With the aim to provide information about system response in cold weather conditions, we first placed a mannequin model with the facemask in the thermal chamber in which the air temperature was maintained at 4–6 °C, while humidity was maintained in the range of 35–50%. After 10 min of stabilization, the heating system was turned on and the temperature was monitored for 20 min. The obtained results are shown in Figure 8a, clearly indicating that wearing the facemask increases air temperature even when the heating system is switched off. More importantly, our heating system provides elevated air temperatures to approximately 38 °C, which is equal to the temperature increase of $\Delta T = 23$ °C. Extreme cold weather conditions were replicated again with the thermal chamber in which air temperature was maintained at –18 °C, while humidity was maintained in the range of 75–

85%. After 10 min of stabilization, the heating system was turned on and the temperature was monitored for 20 min. As it can be seen from Figure 8b, the air temperature increased from –9 °C to much more comfortable 1 °C, which is equal to a temperature increase of 11 °C.

Finally, data transmission over the BLE link to the mobile phone was tested. Because we used the nRF24L01 from the nordic semiconductor as the hardware element for wireless communication, the data sending protocol in our program code of the microcontroller was realized in such a way that compatibility is ensured with the application “nRF Connect for mobile” for the Android operating system, available for free download and noncommercial use from Google Play.³⁴

3.4. Testing and Monitoring of the Heating Process while a Human Volunteer Is Wearing the Facemask with the Heater. Finally, suitability for a human wearing the facemask with the embroidered textile heater was explored (Figure 9a). The thermocouple was sewed to the facemask to ensure a stable and correct position near the nose.

The test procedure was performed in three phases, as shown in Figure 9b. In the first minute, the volunteer was wearing the mask with the battery that powers the heater being disconnected. During that period, the temperature inside the facemask was obtained to be very stable and approximately equal to 33 °C, which can be approximated as the exhaled air temperature. After that, the battery was connected and a sharp increase in temperature could be noticed in the next 6 min. It is important to emphasize that the thermocouple position was slightly changed to provide a more comfortable mask-wearing experience and to avoid a short circuit with the conductive threads of the heater because of the slight change in the face shape of the mannequin model and the volunteer. The two following aspects can be noticed.

First, the temperature inside the facemask is lower when compared to testing with the mannequin model. This can be attributed to the forced air flow of the human exhalation which, by being at approximately 33 °C, effectively cools down

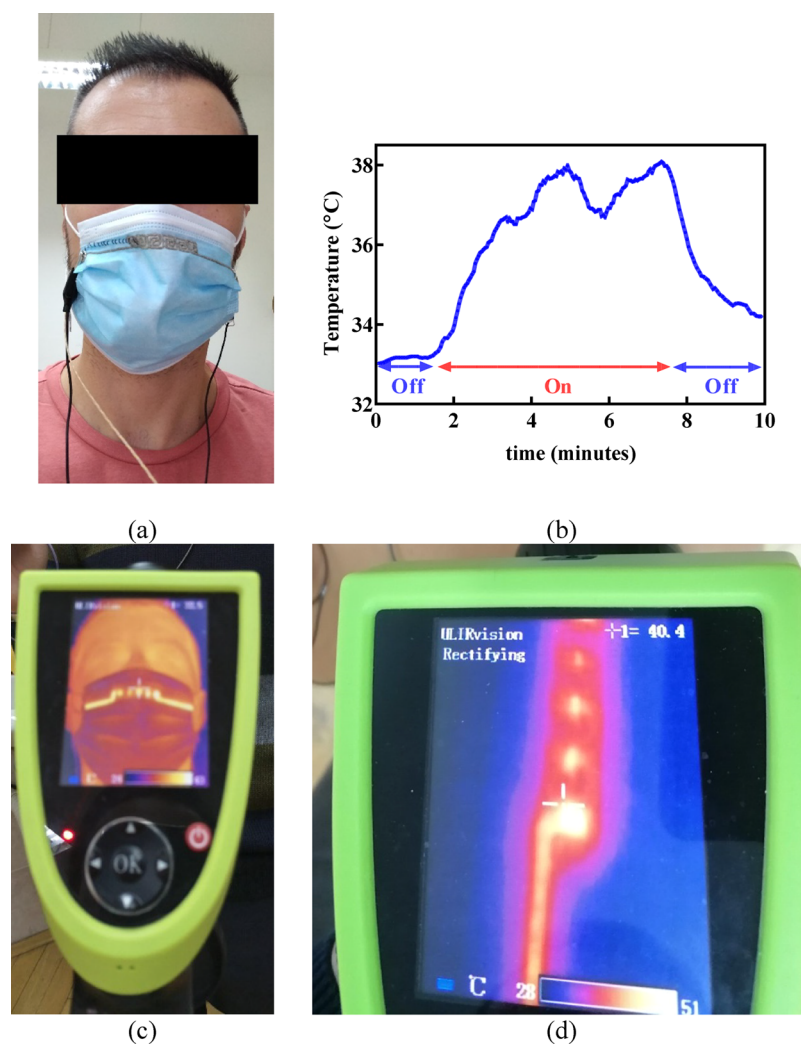


Figure 9. (a) Human volunteer wearing the facemask with the embroidered textile heater, (b) temperature values of the air inside the facemask while the volunteer was wearing the facemask with the embroidered textile heater, (c) safety checks using the thermal (infrared) camera while the user is wearing the facemask, and (d) enlarged details of the thermal camera with a visible scale bar.

the air temperature despite the ongoing heating process. It is possible to obtain a higher temperature of the heater while a volunteer wears the facemask with a simple increase in t_{on} time. However, we limited the heating process as it is very important to prioritize the safety of the user and avoid any burns or discomfort. An additional safety verification was performed using thermal (infrared) camera scanning while the user was wearing the facemask, as it is shown in Figure 9c, indicating a uniform temperature of the textile-based heater.

The second observation from Figure 9b is that in the middle of the test, a small temperature drop can be seen. This is because the heating process was reduced to 40% of the total time (Table 2), enabling the decrease of air temperature during breathing. However, in less than 15 s, the air temperature increased again to the stable value.

3.5. Efficiency of Energy Conversion with the Proposed Textile Heater and Temperature-Regulating Circuit. As the final verification part of the proposed system with the textile heater, we performed a power consumption and efficiency analysis. The Sanwa CD770 multimeter was used as an ammeter and connected in series with the battery. The used battery was a standard PP3 9 V alkaline from Maxell.³⁵ As the actual battery capacity varies among




manufacturers and different storage conditions, we chose to characterize the abovementioned type of battery but without the longevity test as it cannot be generalized for batteries of different capacities and states of health. In this work, we focus on the power consumption and efficiency analysis, which can be later used for a more precise performance estimation of some specific battery with the given capacity. In the standby mode, with the MOSFET turned off, the current consumption is 6.6 mA, while in the active mode, when the MOSFET is on, the current consumption is close to 210 mA. Thus, the power consumption P from the battery is

$$P = \begin{cases} 59.4 \text{ mW, standby mode} \\ 1890 \text{ mW, active mode} \end{cases} \quad (1)$$

Keeping in mind that the heater resistance, measured with the multimeter at the ambient temperature of 30 °C, was about 27.42 Ω , and that the voltage level at the heater is 5 V, the power efficiency of the proposed heating system is as follows:

$$\text{Efficiency (\%)} = \frac{\frac{(5 \text{ V})^2}{27.42 \text{ } \Omega}}{9 \text{ V} \times 210 \text{ mA}} \times 100\% = 51\% \quad (2)$$

Table 5. Performance Comparison of the Developed System with the State-of-the-Art^a

Ref. year Parameter	²⁵ , 2021	²⁷ , 2021	This work
Size (all in mm)	20 × 20	80 × 60	9.2 × 197.6
Weight (g)	NR	NR	3
Temperature (°C)	43	40	44
Power (W)	NR	3.79	1.89
Flexible	Partially	No	Yes
Electronic feedback for temperature regulation	No	No	Yes
Photo illustration			
	This photo is reproduced with permission from ref. ²⁵ . Copyright 2022 American Chemical Society.	This photo is reproduced with permission from ref. ²⁷ . Copyright 2021 American Institute of Chemical Engineers.	
Price (EUR)	NR	NR	0.5

^aNR – not reported.

which was expected because of the amount of the energy dissipated on the voltage regulator (IC7805) with voltage regulation from 9 to 5 V. One possible solution for this can be the use of a more efficient switching-type voltage regulator, which we will explore in the future work. Moreover, the use of external power banks with 5 V output which is applied directly to the heater and controlled with our electronics is another solution as that would remove the need for internal voltage reduction. It is also important to notice that the efficiency is about to decrease with increasing electrical resistance because of the increased temperature. However, when air temperature is increased due to the increased heater temperature, the battery will spend most of the time in standby mode which will decrease the power consumption.

3.6. Performance Comparison of the Developed System with the State-of-the-Art. Key performance indicators (KPIs) of the proposed system and comparison with the state-of-the-art are given in Table 5. Much to regret, some of the important parameters (such as weight and price) are not reported in relevant references.

The main contributions and novelty of our realization can be summarized as follows: (1) all components of the system are commercially available, which eliminates need for the complex and expensive production process, (2) the proposed system offers a fully-flexible solution that is compatible with the body shape of people of different age and sex, (3) antibacterial properties of silver that make safe the contact with the human skin, (4) the total weight of the textile heaters which is just 3 grams, (5) it requires less than 50% of power when compared to work presented by Faucher et al.,²⁷ (6) it is the first reported closed-loop solution with autonomous temperature measurement and regulation, (6) the total cost of the materials needed for the realization of the heater structure is less than 0.5 EUR, while the cost of the electronic module for temperature monitoring and regulation is about 90 EUR (50 EUR without TFT display) for small-scale production, and (7) additional sensing opportunities are easily achievable with textile sensors

integration to the facemask, such as capacitive respiration monitoring sensors.²⁹

The same electronic module can be used for different types of facemasks, as well as among different users. For example, family members can share the same electronic module with their own facemasks. Different types of facemasks (single-use and multi-use) are compatible with the presented technology, which means that on any type of textile-based mask, we can embroider a similar heater, which will allow multiple usage of the same textile mask with heating properties.

Another advantage of the proposed design is that previously used facemasks without heaters, after sterilization, can be used again in our production cycle, and heaters can be embroidered without requirements for some special and complex chemical treatments. In addition to that, recently presented technology is capable of converting discarded masks (which may contain our heaters) into batteries that can be used in household devices.³⁶

4. CONCLUSIONS

In this work, for the first time, textile heaters based on commercial conductive threads with appropriate temperature-monitoring and -controlling elements are presented. The presented results indicated suitability of the proposed system architecture for safe human use, which is of great importance for various fields such as personal heating systems and thermotherapy, as well as other health protection and management applications. The expected lifetime of the presented system is primarily limited by the recommendation that a used facemask should be worn up to 4–5 h. However, the heater structure and the designed electronics did not show any changes in tests presented in this paper.

In future work, our focus will be on testing the larger number of volunteers as well as optimizing the heater design to meet higher energy efficiency levels. Another possible direction could be the development of self-powered heating systems that will use energy harvested from body motions or body heat. However, available technology for energy harvesting is still

capable of generating relatively small amounts of energy (thermoelectric generators provide up to 3.8 mW cm⁻² and pyroelectric generators up to 5.8 mW³⁷) that might not be enough for heating in cold weather conditions. It is more appropriate to power sensors and data transmission modules from energy harvesting, but this field is evolving in recent years and progress can be expected. Additionally, we will embroider heaters on masks which are for multiple usage and which can be washed many times along with the heater.

AUTHOR INFORMATION

Corresponding Author

Mitar Simić – Faculty of Technical Sciences, University of Novi Sad, 21000 Novi Sad, Serbia; orcid.org/0000-0002-8300-022X; Email: mitar.simic@uns.ac.rs

Authors

Adrian K. Stavrakis – Faculty of Technical Sciences, University of Novi Sad, 21000 Novi Sad, Serbia

Goran M. Stojanović – Faculty of Technical Sciences, University of Novi Sad, 21000 Novi Sad, Serbia

Complete contact information is available at:
<https://pubs.acs.org/10.1021/acsomega.2c06431>

Author Contributions

The manuscript was written through contributions of all authors. All authors have given approval to the final version of the manuscript.

Notes

The authors declare no competing financial interest.

ACKNOWLEDGMENTS

This research was funded through the European Union's Horizon 2020 research and innovation programme under grant agreement No. 854194, as well as the Provincial Secretariat for Higher Education, Scientific and Research Activity with Project no. 142-451-1820/2022-01/1.

REFERENCES

- (1) Lane, K.; Ito, K.; Johnson, S.; Gibson, E.; Tang, A.; Matte, T. Burden and Risk Factors for Cold-Related Illness and Death in New York City. *Int. J. Environ. Res. Public Health* **2018**, *15*, 632.
- (2) Yang, J.; Zhou, M.; Li, M.; Yin, P.; Wang, B.; Pilot, E.; Liu, Y.; van der Hoek, W.; van Asten, L.; Krafft, T.; Liu, Q. Diurnal Temperature Range in Relation to Death from Stroke in China. *Environ. Res.* **2018**, *164*, 669–675.
- (3) Polcaro-Pichet, S.; Kosatsky, T.; Potter, B. J.; Bilodeau-Bertrand, M.; Auger, N. Effects of Cold Temperature and Snowfall on Stroke Mortality: A Case-Crossover Analysis. *Environ. Int.* **2019**, *126*, 89–95.
- (4) Amirkhani, M.; Ghaemimood, S.; von Schreeb, J.; El-Khatib, Z.; Yaya, S. Extreme Weather Events and Death Based on Temperature and CO₂ Emission – A Global Retrospective Study in 77 Low-, Middle- and High-Income Countries from 1999 to 2018. *Prev. Med. Rep.* **2022**, *28*, No. 101846.
- (5) Dangers of Breathing Cold Air, <https://Coldavenger.Com/Blogs/News/18037160-Dangers-of-Breathing-Cold-Air>, (accessed on September 14, 2022).
- (6) D'Amato, M.; Molino, A.; Calabrese, G.; Cecchi, L.; Annesi-Maesano, I.; D'Amato, G. The Impact of Cold on the Respiratory Tract and Its Consequences to Respiratory Health. *Clin. Transl. Allergy* **2018**, *8*, 20.
- (7) Komolafe, A.; Zaghari, B.; Torah, R.; Weddell, A. S.; Khanbareh, H.; Tsikriteas, Z. M.; Vousden, M.; Wagih, M.; Jurado, U. T.; Shi, J.; Yong, S.; Arumugam, S.; Li, Y.; Yang, K.; Savelli, G.; White, N. M.; Beeby, S. E-Textile Technology Review—From Materials to Application. *IEEE Access* **2021**, *9*, 97152–97179.
- (8) Faruk, M. O.; Ahmed, A.; Jalil, M. A.; Islam, M. T.; Shamim, A. M.; Adak, B.; Hossain, M. M.; Mukhopadhyay, S. Functional Textiles and Composite Based Wearable Thermal Devices for Joule Heating: Progress and Perspectives. *Appl. Mater. Today* **2021**, *23*, No. 101025.
- (9) Zhang, L.; Baima, M.; Andrew, T. L. Transforming Commercial Textiles and Threads into Sewable and Weavable Electric Heaters. *ACS Appl. Mater. Interfaces* **2017**, *9*, 32299–32307.
- (10) Kwon, H.; Ul Hassan, N.; Lee, B. Toward an Inductively Powered Wearable Heater Using Conductive Thread Coil. In *2020 IEEE PELS Workshop on Emerging Technologies: Wireless Power Transfer (WoW)*; IEEE: Seoul, Korea (South), 2020; pp 242–245.
- (11) Shahariar, H.; Kim, I.; Bhakta, R.; Jur, J. S. Direct-Write Printing Process of Conductive Paste on Fiber Bulks for Wearable Textile Heaters. *Smart Mater. Struct.* **2020**, *29*, No. 085018.
- (12) Wu, S.; Cui, Z.; Baker, G. L.; Mahendran, S.; Xie, Z.; Zhu, Y. A Biaxially Stretchable and Self-Sensing Textile Heater Using Silver Nanowire Composite. *ACS Appl. Mater. Interfaces* **2021**, *13*, 59085–59091.
- (13) Hong, S.; Lee, H.; Lee, J.; Kwon, J.; Han, S.; Suh, Y. D.; Cho, H.; Shin, J.; Yeo, J.; Ko, S. H. Highly Stretchable and Transparent Metal Nanowire Heater for Wearable Electronics Applications. *Adv. Mater.* **2015**, *27*, 4744–4751.
- (14) Liu, X.; Jin, X.; Li, L.; Wang, J.; Yang, Y.; Cao, Y.; Wang, W. Air-Permeable, Multifunctional, Dual-Energy-Driven MXene-Decorated Polymeric Textile-Based Wearable Heaters with Exceptional Electrothermal and Photothermal Conversion Performance. *J. Mater. Chem. A* **2020**, *8*, 12526–12537.
- (15) Wang, Q.-W.; Zhang, H.-B.; Liu, J.; Zhao, S.; Xie, X.; Liu, L.; Yang, R.; Koratkar, N.; Yu, Z.-Z. Multifunctional and Water-Resistant MXene-Decorated Polyester Textiles with Outstanding Electromagnetic Interference Shielding and Joule Heating Performances. *Adv. Funct. Mater.* **2019**, *29*, No. 1806819.
- (16) Wang, X.; Lei, Z.; Ma, X.; He, G.; Xu, T.; Tan, J.; Wang, L.; Zhang, X.; Qu, L.; Zhang, X. A Lightweight MXene-Coated Nonwoven Fabric with Excellent Flame Retardancy, EMI Shielding, and Electrothermal/Photothermal Conversion for Wearable Heater. *Chem. Eng. J.* **2022**, *430*, No. 132605.
- (17) Gozutok, Z.; Agirbas, O.; Bahtiyari, M. I.; Ozdemir, A. T. Low-Voltage Textile-Based Wearable Heater Systems Fabricated by Printing Reactive Silver Inks. *Sens. Actuators, A* **2021**, *322*, No. 112610.
- (18) Shin, Y.-E.; Cho, J. Y.; Yeom, J.; Ko, H.; Han, J. T. Electronic Textiles Based on Highly Conducting Poly(Vinyl Alcohol)/Carbon Nanotube/Silver Nanobelt Hybrid Fibers. *ACS Appl. Mater. Interfaces* **2021**, *13*, 31051–31058.
- (19) Ahmed, A.; Jalil, M. A.; Hossain, M. M.; Moniruzzaman, M.; Adak, B.; Islam, M. T.; Parvez, M. S.; Mukhopadhyay, S. A PEDOT:PSS and Graphene-Clad Smart Textile-Based Wearable Electronic Joule Heater with High Thermal Stability. *J. Mater. Chem. C* **2020**, *8*, 16204–16215.
- (20) Wang, B.; Yang, K.; Cheng, H.; Ye, T.; Wang, C. A Hydrophobic Conductive Strip with Outstanding One-Dimensional Stretchability for Wearable Heater and Strain Sensor. *Chem. Eng. J.* **2021**, *404*, No. 126393.
- (21) Tian, T.; Wei, X.; Elhassan, A.; Yu, J.; Li, Z.; Ding, B. Highly Flexible, Efficient, and Wearable Infrared Radiation Heating Carbon Fabric. *Chem. Eng. J.* **2021**, *417*, No. 128114.
- (22) Li, Y.; Zhang, Z.; Li, X.; Zhang, J.; Lou, H.; Shi, X.; Cheng, X.; Peng, H. A Smart, Stretchable Resistive Heater Textile. *J. Mater. Chem. C* **2017**, *5*, 41–46.
- (23) Souri, H.; Bhattacharyya, D. Wool Fabrics Decorated with Carbon-Based Conductive Ink for Low-Voltage Heaters. *Mater. Adv.* **2022**, *3*, 3952–3960.
- (24) Salam, B.; Soo, G. C. Y.; Shan, X. C.; Lok, B. K. Washability of Flexible Printed Circuitry for Wearable Electronics Applications. In *2020 IEEE 22nd Electronics Packaging Technology Conference (EPTC)*; IEEE: Singapore, 2020; pp 207–209.

- (25) Han, S.; Kim, J.; Lee, Y.; Bang, J.; Kim, C. G.; Choi, J.; Min, J.; Ha, I.; Yoon, Y.; Yun, C.-H. Transparent Air Filters with Active Thermal Sterilization. *Nano Lett.* **2022**, *22*, 524–532.
- (26) Shin, J.; Jeong, S.; Kim, J.; Choi, Y. Y.; Choi, J.; Lee, J. G.; Kim, S.; Kim, M.; Rho, Y.; Hong, S.; Choi, J. I.; Grigoropoulos, C. P.; Ko, S. H. Dynamic Pore Modulation of Stretchable Electrospun Nanofiber Filter for Adaptive Machine Learned Respiratory Protection. *ACS Nano* **2021**, *15*, 15730–15740.
- (27) Faucher, S.; Lundberg, D. J.; Liang, X. A.; Jin, X.; Phillips, R.; Parviz, D.; Buongiorno, J.; Strano, M. S. A Virucidal Face Mask Based on the Reverse-flow Reactor Concept for Thermal Inactivation of SARS-CoV-2. *AIChE J.* **2021**, *67*, No. e17250.
- (28) Stavrakis, A. K.; Simić, M.; Stojanović, G. M. Electrical Characterization of Conductive Threads for Textile Electronics. *Electronics* **2021**, *10*, 967.
- (29) Simić, M.; Stavrakis, A. K.; Sinha, A.; Premčevski, V.; Markoski, B.; Stojanović, G. M. Portable Respiration Monitoring System with an Embroidered Capacitive Facemask Sensor. *Biosensors* **2022**, *12*, 339.
- (30) Company DIS Export – Import Belgrade, Serbia.
- (31) Qureshi, S.; Stojanović, G. M.; Simić, M.; Jeoti, V.; Lashari, N.; Sher, F. Silver Conductive Threads-Based Embroidered Electrodes on Textiles as Moisture Sensors for Fluid Detection in Biomedical Applications. *Materials* **2021**, *14*, 7813.
- (32) Payne-James, J.; Byard, R. W.; Corey, T. S. Encyclopedia of Forensic and Legal Medicine. *J. Leg. Med.* **2006**, *27*, 361–366.
- (33) Mechanical Engineers Develop Heated Face Masks to Kill Viruses and Curb Disease Spread, <https://www.mae.ucla.edu/mechanical-engineers-develop-heated-face-masks-to-kill-viruses-and-curb-disease-spread/>, 2021, (accessed on June 30, 2022).
- (34) NRF Connect for Mobile, <https://play.google.com/store/apps/details?id=no.nordicsemi.android.mcp&hl=sr&gl=US>, (accessed on June 30, 2022).
- (35) 6LR61 9 Volt Blister 1 Pk, <https://www.maxell.eu/product/6lr61-9-volt-blister-1-pk/>, (accessed on June 30, 2022).
- (36) Batteries Made from Recycled Face Masks, <https://www.springwise.com/innovation/sustainability/batteries-made-from-recycled-masks>, (accessed on September 15, 2022).
- (37) Zou, Y.; Bo, L.; Li, Z. Recent Progress in Human Body Energy Harvesting for Smart Bioelectronic System. *Fundam. Res.* **2021**, *1*, 364–382.